ACS APPLIED MATERIALS & INTERFACES

Research Article

Cite This: ACS Appl. Mater. Interfaces 2019, 11, 38929−38936

www.acsami.org

Stable Subloop Behavior in Ferroelectric Si-Doped HfO_2

Kyoungjun Lee,[†,▽] Hyun-Jae Lee,[§,▽] Tae Yoon Lee,[†] Hong Heon Lim,[†] Myeong Seop Song,[†] Hyang Keun Yoo,[∥] Dong Ik Suh,[∥] Jae Gil Lee,[∥] Zhongwei Zhu,[⊥] Alexander Yoon,[⊥] Matthew R. MacDonald,[#] Xinjian Lei,[#] Kunwoo Park,[‡,¶] Jungwon Park,[‡,¶] Jun Hee Lee,*[,§] and Seung Chul Chae*[,†]

[†]Department of Physics Education and [‡]School of Chemical and Biological Engineering, Institute of Chemical Process, Seoul National University, Seoul 08826, Korea

[§]School of Energy and Chemical Engineering, Ulsan National Institute of Science and Technology (UNIST), Ulsan 44919, Korea

[∥]SK Hynix Incorporation, Icheon-si, Gyeonggi-do 17336, Korea

[⊥]Lam Research Corporation, Fremont, California 94538, United States

[#]Versum Materials Incorporation, Carlsbad, California 92011, United States

[¶]Center for Nanoparticle Research, Institute for Basic Science (IBS), Seoul 08826, Korea

Supporting Information

ABSTRACT: The recent demand for analogue devices for neuromorphic applications requires modulation of multiple nonvolatile states. Ferroelectricity with multiple polarization states enables neuromorphic applications with various architectures. However, deterministic control of ferroelectric polarization states with conventional ferroelectric materials has been met with accessibility issues. Here, we report unprecedented stable accessibility with robust stability of multiple polarization states in ferroelectric HfO_2. Through the combination of conventional voltage measurements, hysteresis temperature dependence analysis, piezoelectric force microscopy, first-principles calculations, and Monte Carlo simulations, we suggest that the unprecedented stability of intermediate states in ferroelectric HfO_2 is due to the small critical volume size for nucleation and the large activation energy for ferroelectric dipole flipping. This work demonstrates the potential of ferroelectric HfO_2 for analogue device applications enabling neuromorphic computing.

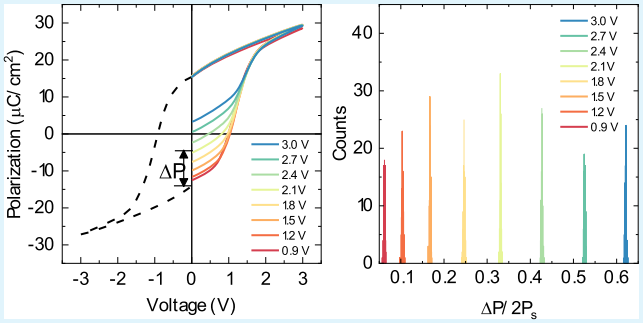

KEYWORDS: *FeRAM, ferroelectric, multilevel, analogue device, HfO_2*

INTRODUCTION

The massive demand for versatile analogue devices in neuromorphic computing is a major issue for artificial intelligence applications. Machine learning and deep learning, based on both discriminative and generative models, require a neural network that includes memory, a memory-read/write head, state register, and memory write rules with analogue weight and bias parameters. From an analogue perspective, conceptual devices with multiple nonvolatile states for multiply-accumulate operations have been proposed through hardware implementation that replaces the data transfer of weight and bias values with a bus between the physical memory and processor.[1,2] To this end, various architectures can be constructed based on a ferroelectric framework, in which partial polarization switching is possible. For example, variable ferroelectric polarization in conventional devices involving stacked ultrathin films can be used for tunneling junctions with multiple resistance states.[3,4] In addition, modulation of the physical properties of matter by the ferroelectric field effect with analogue polarization values has been proposed for single-transistor architectures in nonvolatile memory.[5] Irrespective of the mechanisms used for data storage modulation, explicit control of ferroelectric polarization switching, especially unsaturated ferroelectric polarization hysteresis subloops, is a key factor in achieving the desired properties in these analogue devices.

Recently, diverse approaches to achieve stable subloop polarization states have been demonstrated through the external circuit element and material's internal or external factors. The external circuit elements such as transistors which limit undergoing current control the portion of the ferroelectric domain flipping via restraint of the ferroelectric domain wall motion and/or nucleation processes.[6] However, the compliance level of transistors is beyond the contemporary

Received: July 22, 2019
Accepted: October 2, 2019
Published: October 2, 2019

DOI: 10.1021/acsami.9b12878
ACS Appl. Mater. Interfaces 2019, 11, 38929−38936

specification of memory device applications, in which scaling problems and additional resistive−capacitance delay (e.g., in memory cell transistors) present complications with respect to achieving optimal device performance.[7,8] On the other hand, although the mediation of the material's external factors such as interfacial layer[9] or defect dipoles[10] enabled the multilevel polarization states, the artifacts raised the fatigue and imprint problems.[11,12] The control of the material's internal structural variants through multilayer heterostructure,[13,14] structural instability[15,16] or ferroelastic twin domains[17,18] achieved multilevel polarization states. However, these approaches are constrained by the limited number of switching states or incontrollable twin domains due to the predefined electrostatic energies.[19,20]

Considering the broken inversion symmetry of ionic configurations, an external electric field is a direct external stimulus for macroscopic ferroelectric switching. With respect to the magnitude of the external electric bias, systematic variation of the ferroelectric polarization can be achieved, leaving behind many or continuous intermediate polarization states. To control the polarization precisely, active modulation of the amplitude, duration, and/or repetition of an external stimulus has been considered. However, because of the complicated switching mechanism of ferroelectrics and/or defect-induced uncertainties,[21−23] multiple attempts using the aforementioned stimuli have yet to reach finite analogue states with the desired accuracy without the cost of delayed switching, fatigue, or imprint problem. In addition, this instability of multilevel polarization states is worsened in small material volumes, inhibiting practical downscaled device application.[21]

Recently, hafnium (Hf)-based ferroelectrics have attracted much attention, due not only to their compatibility with current complementary metal−oxide−semiconductor (CMOS) technology but also their use as an alternative to perovskite ferroelectrics.[24−27] Despite having a large spontaneous polarization, perovskite materials have struggled with poor compatibility with CMOS technology and switching limitations because of their small band gap and oxygen instability. However, since the discovery of ferroelectricity in HfO_2, subsequent investigations have revealed the robust switching behavior of this material.[28−30] In tunneling junction devices and ferroelectric field-effect transistors, polarization switching stability has been investigated extensively, with regard to the structural integrity of the material and its switching mechanism. Prior results have shown a large polarization in HfO_2, comparable to those of $Pb(Zr_xTi_{1-x})O_3$ (PZT) and $BaTiO_3$; additionally, HfO_2 has shown the ability to maintain polarization under retention and fatigue testing.[26,29] In addition, the subloop polarization in ferroelectric HfO_2-based memory architectures demonstrated empirical deterministic control of memory states with advantages for neuromorphic applications such as low-power consumption.[31−37] Considering thin-film thickness (∼10 nm) and polycrystalline structure-induced defects of ferroelectric HfO_2, deterministic control of multilevel polarization states is remarkable. However, the direct study of stability in multilevel polarization states in ferroelectric HfO_2 capacitors and the origin of deterministic control is insufficient (i.e., reproducibility and retention of multilevel polarization states). Prior to analogue device application, direct investigation of the subloop behavior in ferroelectric HfO_2 is urgently required.

In this study, we report unprecedented stability in the subloop switching behavior and accessibility to intermediate polarization states in ferroelectric Si-doped HfO_2. We suggest that the enhanced stability of the intermediate states is due to the small critical volume for ferroelectric nucleation in HfO_2 and the large activation energy for flipping the polarization dipole. Conventional voltage pulse measurements, an analysis of the temperature dependence of hysteresis, and piezoresponse force microscopy (PFM) measurements were conducted to confirm the small volume for ferroelectric nucleation with large activation energy per unit volume. Theoretical calculations were used to investigate the switching energy landscape of ferroelectric HfO_2. Monte Carlo simulation results confirmed the existence of stable multilevel states, with accessibility facilitated by the small nucleation volume.

EXPERIMENTAL SECTION

Sample Fabrication. The 4.2 mol% Si-doped HfO_2 films (thickness: 8 nm) were stacked on the TiN bottom electrode, using the atomic layer deposition process based on tetrakis(dimethylamido)hafnium (TDMAH), tetrakis(dimethylamino)silane (4DMAS), and ozone.[38] For the electrical measurements, the Pt/TiN top electrode was patterned with a circular shape radius of 100 μm. To crystallize the Si-doped HfO_2, post annealing was conducted at 600 °C for 20 s in N_2 ambient conditions after the deposition of the top electrode known as the post metallization annealing.

Electric Measurement. Polarization−voltage (P−V) curves and time-dependent dynamic polarization switching $P(t)$ were assessed using a ferroelectric tester (TF Analyzer 3000; aixACCT Systems GmbH, Aachen, Germany) and a rapid data acquisition system (4200-SCS; Keithley Instruments, Cleveland, OH, USA). All electric measurements were performed after the wake-up process, by inducing 10 000 voltage pulse cycles of 3 V at a frequency of 10 kHz.

Ferroelectric Domain Imaging. Local polarization switching was measured via PFM (Cypher; Asylum Research, Santa Barbara, CA, USA) with a conventional platinum/iridium-coated tip (PPP-EFM; NANOSENSORS, Neuchatel, Switzerland).

RESULTS AND DISCUSSION

Ferroelectric HfO_2 exhibits manifold polarization states, applicable for use in analogue devices. Figure 1a shows the multilevel polarization states through the positive region of the polarization−voltage (P−V) hysteresis loops. These intermediate states can be manipulated by simply varying the amplitude of the external bias. We controlled the multilevel polarization states of our HfO_2 sample by applying voltage pulses of different magnitudes over the range of 0.9−3 V, within a fixed window of 2 μs. The voltage pulses were applied initially to a negatively polled sample, in which the intermediate polarization states were measured with a triangular pulse of 3 V and a frequency of 2 kHz. The term ΔP in Figure 1a refers to the difference between the remnant polarization value of intermediate states and the fully negatively polled state. ΔP increased systematically with the voltage. These results suggest that voltage variation can be used to control the intermediate states of ferroelectric HfO_2, in which the analogue behavior of ΔP can be used as a synaptic weight in neuromorphic computing (Supporting Information, Section S3).

The inherent multiplicity of HfO_2 ferroelectric polarization states was maintained with discernible accuracy with repeated application of external voltage pulses. The reliability of an intermediate polarization state was determined by its reproducibility and retention properties. To confirm reprodu-

DOI: 10.1021/acsami.9b12878
ACS Appl. Mater. Interfaces 2019, 11, 38929−38936

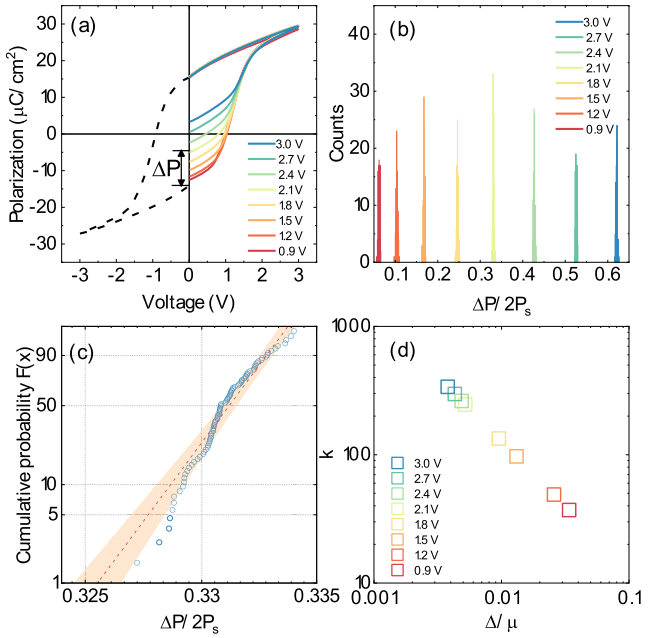

Figure 1. Multilevel states and reliability of Si-doped HfO_2 thin films. (a) Intermediate polarization states of ferroelectric HfO_2 using 2 μs voltage pulses. (b) Histogram of each intermediate polarization state repeated 100 times. (c) Weibull statistic fitting reliability results of the intermediate polarization states using 2.1 V, 2 μs voltage pulses with orange-shaded 95% confidence interval. (d) Statistic results of each intermediate polarization states in terms or Weibull exponent value k and the standard deviation to mean ratio Δ/μ.

cibility, we repeated each voltage pulse sequence 100 times and measured the $\Delta P/2P_s$ values for a particular intermediate state; the measurement results are shown as a histogram in Figure 1b. The measured $\Delta P/2P_s$ had a narrow standard deviation of less than 0.003, and the separation among states exceeded 0.03. Note that typical perovskite ferroelectric materials show unstable reproducibility with conventional voltage/field control;[6] in contrast, the ferroelectric HfO_2 film showed reliable reproducibility with high accuracy.

For the detailed analysis of the reproducibility of each intermediate states, we analyzed the statistics in terms of the Weibull distribution as shown in Figure 1c by the following equation

$$F(x) = 1 - \exp[-(x/x_0)^k) \quad (1)$$

$F(x)$ is the cumulative probability of randomly distributed variable ($\Delta P/2P_s$ value in this work), x is the random variable, x_0 is the scale parameter, and k is the Weibull exponent. The Weibull exponent value k is correlated with the standard deviation to mean ratio Δ/μ as follows

$$\Delta/\mu = \frac{[\Gamma(1 + 2/k) - \Gamma^2(1 + 1/k)]^{1/2}}{\Gamma(1 + 1/k)} \quad (2)$$

where Γ is the Gamma function. Each intermediate polarization states exhibited a large k value ranging from 37.1 to 338 as shown in Figure 1d. Note that our results exhibited a large k value with small Δ/μ compared to the reported ferroelectric tunnel junction devices[39] and even comparable with the contemporary other mersister devices,[40] indicating superior reproducibility.

The robust stability of each manifold state of ferroelectric HfO_2 was observed under high-temperature and is considered as the device operation environment. To confirm the retention properties of the material, we examined the time evolution of $\Delta P/2P_s$. Figure 2a shows the retention of intermediate

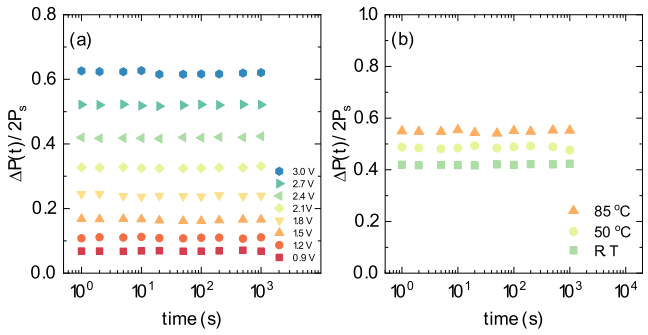

Figure 2. (a) Retention properties of each intermediate polarization state of ferroelectric HfO_2 measured at room temperature. (b) Retention properties of an intermediate state, using 2.4 V, 2 μs voltage pulses at room temperature, 50 and 85 °C.

polarization states at room temperature; the polarization was sustained, with only a slight loss after 1000 s. Figure 2b shows the intermediate state retention with 2.4 V, 2 μs pulses at room temperature, 50, and 85 °C. The polarization loss observed at 50 and 85 °C showed only a slight difference with respect to the pristine state after 1000 s, as shown in Figure 2b. The time evolution of intermediate polarization under voltage pulse application exhibited long-term stability, a requirement for practical applications.

The unprecedented stability of the polarization states in HfO_2 can be understood in terms of ferroelectric switching dynamics and the underlying mechanism responsible for deterministic control of the polarization via a large coercive field. Figure 3a shows the time and voltage dependences of ferroelectric polarization in the Si:HfO_2 thin film; the solid dots represent the experimental polarization switching with different applied voltages ranging from 0.9 to 3.0 V. To estimate the time evolution of polarization switching, the portion of switched polarization was measured after applying a positive pulse to the top electrode, with a subsequent increase in the pulse width and height. Before inducing a positive pulse, a negative pulse was introduced with a height and width of −3 V and 125 μs, respectively, at the top electrode for full saturation (Supporting Information, Section S5). The solid lines in Figure 3a represent the fitting results obtained using a nucleation-limited switching (NLS) model, with a Lorentzian distribution for the characteristic switching time as below.[41]

$$\frac{\Delta P(t)}{2P_s} = \int_{-\infty}^{\infty} \left\{1 - \exp\left[-\left(\frac{t}{t_0}\right)^2\right]\right\} F(\log t_0)\mathrm{d}(\log t_0) \quad (3)$$

where

$$F(\log t_0) = \frac{A}{\pi}\left[\frac{w}{(\log t_0 - \log t_1)^2 + w^2}\right] \quad (4)$$

A, w, and $\log t_1$ indicate a normalization constant, the half width at half-maximum of the distribution, and the mean value of the distribution, respectively.

DOI: 10.1021/acsami.9b12878
ACS Appl. Mater. Interfaces 2019, 11, 38929−38936

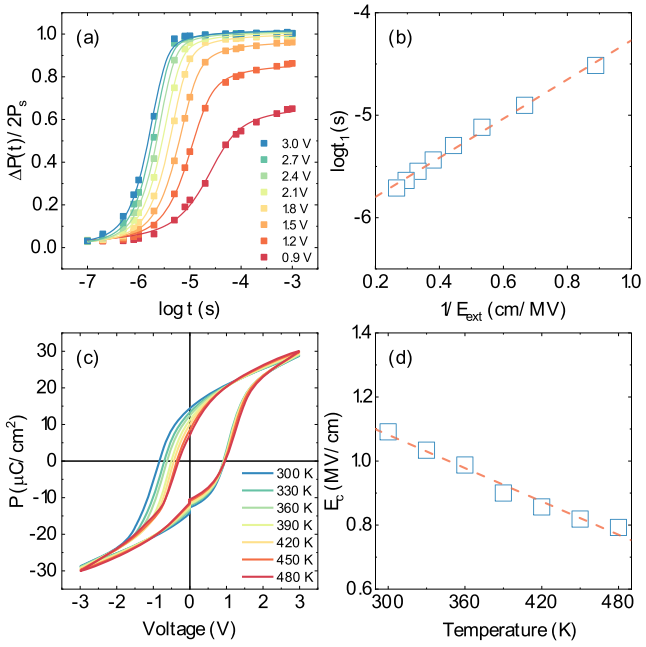

Figure 3. Ferroelectric switching dynamics and temperature dependence of ferroelectric hysteresis. (a) Time and voltage dependence of the switched polarization $\Delta P(t)$ measured at room temperature. The solid lines represent the fitting results using the NLS model, considering the Lorentzian distribution of the characteristic switching time for ferroelectric nucleation. (b) External voltage dependence of the characteristic switching time. (c) Temperature dependence of ferroelectric hysteresis. (d) Temperature dependence of the coercive field.

Figure 3b shows the characteristic switching time estimated from the position of the Lorentzian peak. The linear dependence in Figure 3b reveals the ferroelectric properties associated with nucleation and domain wall propagation.[42] The activation field was estimated to be 1.9 MV/cm, which is similar to a recently reported value in a Zr-doped ferroelectric HfO_2 film.[43] It is worth noting that the activation field for ferroelectric switching in HfO_2 is larger than those of other perovskite ferroelectrics,[44−46] enabling long-term stability of intermediate states due to the high coercive field.[47−49]

To understand the large activation field associated with the nucleation energy per unit volume and the critical volume size of nucleation, we examined the temperature dependence of the coercive field, with a focus on the barrier height for ferroelectric switching in HfO_2 films. Figure 3c shows the temperature dependence of the ferroelectric hysteresis from 300 to 480 K, with the application of 3 V pulses at a frequency of 2 kHz. Because of the different concentrations of trap sites and/or oxygen vacancies at the bottom and top electrode ferroelectric interfaces, the imprint effects were enhanced as the temperature increased.[50] Also, as the measurement temperature increased, the remnant polarization and coercive field decreased. In the classical Landau−Devonshire free-energy model,[51] the variation of the coercive field under varying temperature can be associated with the critical volume and activation energy. The free-energy model can be used to derive the coercive field, barrier height, and critical nucleation volume, as given below[52]

$$E_c = \frac{W_B}{P_s} - \frac{k_b T}{V^* P_s} \ln\left(\frac{\nu_0 t}{\ln(2)}\right) \quad (5)$$

where W_B, P_s, k_b, T, V^*, ν_0, and t are the energy barrier per unit volume, spontaneous polarization, Boltzmann's constant, temperature, critical volume for nucleation, phonon frequency, and measurement time, respectively. We used the soft-mode phonon frequency and the spontaneous polarization value of 1.16×10^{13} Hz and 41 $\mu C/cm^2$, respectively.[53] Figure 3d shows the experimental temperature dependence of the coercive field and the fitting results obtained with eq 1. For the ferroelectric HfO_2 film, we obtained 4.1×10^{26} eV/m^3 for the energy barrier per unit volume (W_B) and 4.0×10^{-27} m^3 for the critical volume for nucleation (V^*); both are similar to the values obtained in a previous study of Si-doped HfO_2.[54] Note that W_B is larger than that for PZT[55] (PZT: $W_B = 0.38 \times 10^{26}$ eV/m^3, $V^* = 25 \times 10^{-27}$ m^3), which can be attributed to the large coercive field of HfO_2; V^* was much smaller than that for PZT. However, although V^* is small, the energy barrier per critical volume for nucleation ($W_B \times V^*$) of HfO_2 is still larger than that of PZT.

Scanning probe microscopy demonstrated the influence of critical volume size on ferroelectric switching, in terms of the domain wall speed and size. The stable and small critical volume for ferroelectric nucleation is due to the weak interaction between ferroelectric dipoles. There should be little movement of the domain wall with weak interaction and a high activation barrier.[55] To confirm the domain wall motion of ferroelectric HfO_2, we used PFM to estimate the domain wall velocity and its activation field. Figure 4a shows piezoresponse spectroscopy results observed in the HfO_2 thin film; the results showed a clear hysteresis in amplitude and phase, with a local coercivity of ~3 V and phase responses that corresponded to upward/downward polarization, as indicated by the blue circles. Figure 3b−e show out-of-plane directional phase images along the external bias, at different

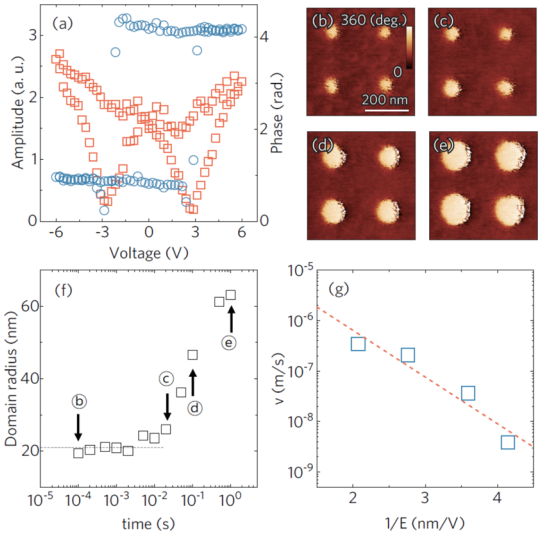

Figure 4. Piezoresponse properties and the speed of ferroelectric domain wall propagation in a Si-HfO_2 thin film using local PFM. (a) Amplitude (empty red square) and phase (empty blue circle) hysteresis of local PFM. (b−e) PFM phase images after positive poling with a pulse height of 6 V and widths of 100 μs, 20 ms, 100 ms, and 1 s, respectively. Before the measurement, the sample was poled with a negative bias of −6 V. (f) Voltage pulse width dependence of the equivalent domain radius for the switched region. The dashed gray line represents the minimum domain size resolution (~20 nm). (g) Electric field dependence of the domain wall velocity.

DOI: 10.1021/acsami.9b12878
ACS Appl. Mater. Interfaces 2019, 11, 38929−38936

pulse widths and with a fixed voltage of 6 V on the negatively pre-polled area. Without any thermally nucleated domains in the scan area, clear domain growth was observed, with dominant domain wall motion, at ~20 nm resolution.

The domain wall velocity and activation energy for the propagation of the domain wall can be estimated using the external pulse width. Figure 4f shows the domain radius as a function of the external pulse width; the domain size was seemingly unchanged along with the external bias, with a width of less than 10 ms. The domain radius increased with the domain wall motion as the bias exceeded 10 ms. This may be due to the minimum size of the domain radius of ~20 nm for the resolution limit. During the estimation of the effective velocity of domain wall propagation, the effective electric field under the tip was calculated from a first-order approximation,[56,57] $E = Va/rd$ where V, a, r, and d represent the voltage, tip radius, domain radius, and film thickness, respectively. Figure 4g shows the domain wall velocity as a function of the reciprocal of the external bias. The velocity, specified as $v \approx \exp(-\alpha/E)$, was used to estimate the activation field of domain wall propagation.[42] The calculated activation field for domain wall motion was ~9.3 MV/cm, which is a much larger value than that required for switching activation (~1.9 MV/cm). Note that the domain wall velocity of other perovskite and poly thin film ferroelectrics such as poly(vinylidene fluoride-*co*-trifluoroethylene) thin films is approximately 4 orders of magnitude faster than that of HfO_2 under the same electric field conditions.[57−59] Even considering the large coercive field of ferroelectric HfO_2, the domain wall velocity was nearly 2 orders of magnitude slower at the same ratio of the applied field to the coercive field. These results well matched those of a recent PFM study of La-doped ferroelectric HfO_2.[60] Thus, the PFM results in this study indicate that the domain wall motion in ferroelectric HfO_2 was a small effect compared with other perovskite ferroelectric materials; this was attributed to the minimal interaction among domains in ferroelectric HfO_2.

Theoretical estimation of the energy difference of the flipping of a single ferroelectric dipole elucidates the stability of small ferroelectric domains. First-principles calculations were performed to estimate the total energy difference of a single flip of a ferroelectric dipole moment in a domain of ferroelectric HfO_2. Figure 5a,b shows a schematic atomic configuration of all domains poled in the upward direction and a domain with one downward directional flip of a single dipole, for a comparison of the total energy. The calculated total energy difference between all domains poled in the upward direction and domains with one downward directional flip in HfO_2 was surprising, at 0.079 eV, with a large barrier height during a dipole flip process of 1.3 eV, as shown in Figure 5c. Notably, the same calculation process of conventional perovskite PTO exhibits a large energy difference of 0.65 eV, with a small barrier height of 0.77 eV. Because of the small value difference between the barrier height and the energy difference after a dipole flip, the flipped dipole easily back-switched, indicating the instability of a single ferroelectric dipole flip in this material. In addition, the calculated total energy difference was negligible, regardless of the number of ferroelectric dipole flips for ferroelectric HfO_2 (Supporting Information, Section S6). Therefore, a small critical nucleation volume of the ferroelectric domain can be stabilized without disturbing ferroelectric dipole neighbors.

The causality between the small critical volume for ferroelectric nucleation and the discernible accuracy of the

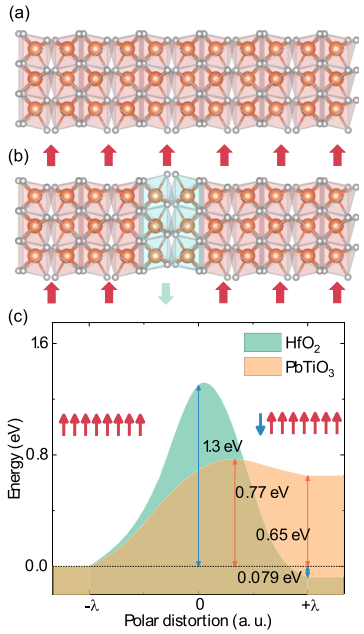

Figure 5. First-principles calculations of a single ferroelectric dipole flip. Schematic diagram of ferroelectric HfO_2 with (a) all upward dipoles and (b) one opposite dipole. (c) Energy landscapes of HfO_2 and $PbTiO_3$ for a single dipole flip.

polarization state was investigated in terms of the critical unit size and the derivation of subloop polarization by Monte Carlo simulations. To elucidate the small domain size effect on multilevel switching, we conducted Monte Carlo simulations of long-range dipole−dipole interactions with a random magnitude of dipole−defect interactions, considering polycrystalline ferroelectric HfO_2.[38,61−63] Figure 6a shows a schematic diagram of the simulation lattice, in which the total length L was fixed and each unit length L/N was varied by the number of mesh grids N. As the number of mesh grids increased, the

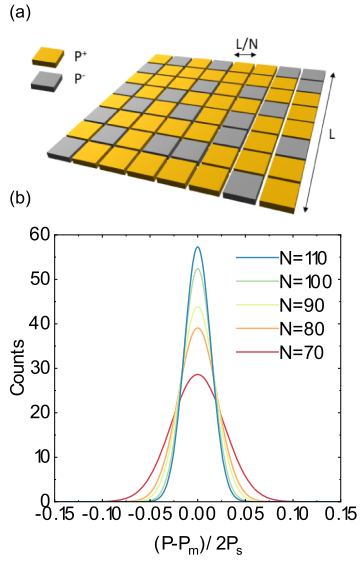

Figure 6. Monte Carlo simulation results with different critical volumes for ferroelectric nucleation. (a) Schematic diagram of the ferroelectric nucleation size at a fixed length divided into a given mesh grid size. (b) Fitted distribution profiles of an intermediate polarization state repeated 100 times for different mesh grid sizes.

DOI: 10.1021/acsami.9b12878
ACS Appl. Mater. Interfaces 2019, 11, 38929−38936

individual domain size decreased. Figure 6b shows the distribution results of polarization switching at a constant Monte Carlo step (MCS) with different numbers of mesh grids repeated 100 times; the distribution profiles were taken at a specific MCS to compare the broadness of accessibility (Supporting Information, Section S7). The constant MCS step corresponds to the experimental characteristic switching time t_0. The numbers of mesh grids are inversely proportional to the size of critical volume for ferroelectric nucleation. The results show the relationship between accessibility to the intermediate states and critical volume for ferroelectric nucleation. As the individual critical volume for ferroelectric nucleation decreased, the intermediate states attained more stable reproducibility.

CONCLUSIONS

Considering the complicated switching mechanism and defect-mediated uncertainty, the stable subloop behavior of ferroelectric HfO_2 with conventional voltage pulses was remarkable. The switching dynamics indicated a large activation field for ferroelectric switching. This large activation field provides robust stability, even at high temperatures, as shown in Figure 2a,b. The temperature dependence of hysteresis and PFM measurements are good indicators of the small size of ferroelectric domains and high activation energy. Theoretical calculations confirmed the large activation energy for a single dipole flip. The stabilization of small-size ferroelectric domain was attributed to the intrinsic stability of a single opposite ferroelectric dipole. Based on the extraordinary stability of small nucleation, the macroscopic discernible accuracy of partial switching of ferroelectricity can be achieved in HfO_2, as shown in Monte Carlo simulation results. Even considering contemporary scaled down device (i.e., 7 nm technology), the small critical volume for nucleation in ferroelectric Si-doped HfO_2 enables diverse multilevel polarization states (more than 32) can be achieved.

In summary, we demonstrated the unprecedented stability of multilevel switching properties in ferroelectric HfO_2. The ferroelectric switching dynamics and temperature dependence of hysteresis elucidate the small activation energy for switching due to the stable and small nucleation size. The associated slow domain wall motion because stable small-sized domains was confirmed by PFM measurements. Monte Carlo simulations demonstrated that the small nucleation size induces stable intermediate polarization states.

ASSOCIATED CONTENT

Supporting Information

The Supporting Information is available free of charge on the ACS Publications website at DOI: 10.1021/acsami.9b12878.

Effects of Si-doping concentration, grain size estimation, synaptic behavior of polarization, details of the experimental method for time-dependent switched polarization, the fitting for polarization switching dynamics, details of theoretical calculation, details of Monte Carlo simulation, supporting results, and figures (PDF)

AUTHOR INFORMATION

Corresponding Authors

*E-mail: junhee@unist.ac.kr (J.H.L.).
*E-mail: scchae@snu.ac.kr (S.C.C.).

ORCID

Kyoungjun Lee: 0000-0003-0472-3583
Tae Yoon Lee: 0000-0003-1754-8657
Jungwon Park: 0000-0003-2927-4331

Author Contributions

$^{\nabla}$K.L. and H.-J.L contributed equally to this work.

Notes

The authors declare no competing financial interest.

ACKNOWLEDGMENTS

This work was supported by the MOTIE (Ministry of Trade, Industry & Energy) (no. 10080657) and KRSC (Korea Semiconductor Research Consortium) support program for the development of future semiconductor devices. Part of this study was performed using facilities at the IBS Center for Correlated Electron Systems, Seoul National University. J.H.L is supported by Creative Materials Discovery Program (2017M3D1A1040828) of NRF. The authors gratefully acknowledge the contributions of all of the joint development members in Lam Research, Versum Materials, and SK Hynix. This paper was the result of the research project supported by SK Hynix Inc.

REFERENCES

(1) Jeong, D. S.; Hwang, C. S. Nonvolatile Memory Materials for Neuromorphic Intelligent Machines. *Adv. Mater.* **2018**, *30*, 1704729.

(2) Upadhyay, N. K.; Jiang, H.; Wang, Z.; Asapu, S.; Xia, Q.; Joshua Yang, J. Emerging Memory Devices for Neuromorphic Computing. *Adv. Mater. Technol.* **2019**, *4*, 1800589.

(3) Chanthbouala, A.; Crassous, A.; Garcia, V.; Bouzehouane, K.; Fusil, S.; Moya, X.; Allibe, J.; Dlubak, B.; Grollier, J.; Xavier, S.; Deranlot, C.; Moshar, A.; Proksch, R.; Mathur, N. D.; Bibes, M.; Barthélémy, A. Solid-State Memories Based on Ferroelectric Tunnel Junctions. *Nat. Nanotechnol.* **2012**, *7*, 101.

(4) Boyn, S.; Grollier, J.; Lecerf, G.; Xu, B.; Locatelli, N.; Fusil, S.; Girod, S.; Carrétéro, C.; Garcia, K.; Xavier, S.; Tomas, J.; Bellaiche, L.; Bibes, M.; Barthélémy, A.; Saïghi, S.; Garcia, V. Learning through Ferroelectric Domain Dynamics in Solid-State Synapses. *Nat. Commun.* **2017**, *8*, 14736.

(5) Wu, S.-Y. A New Ferroelectric Memory Device, Metal-Ferroelectric-Semiconductor Transistor. *IEEE Trans. Electron Devices* **1974**, *21*, 499−504.

(6) Lee, D.; Yang, S. M.; Kim, T. H.; Jeon, B. C.; Kim, Y. S.; Yoon, J.-G.; Lee, H. N.; Baek, S. H.; Eom, C. B.; Noh, T. W. Multilevel Data Storage Memory Using Deterministic Polarization Control. *Adv. Mater.* **2012**, *24*, 402−406.

(7) Auth, C.; Cappellani, A.; Chun, J.; Dalis, A.; Davis, A.; Ghani, T.; Glass, G.; Glassman, T.; Harper, M.; Hattendorf, M.; Hentges, P.; Jaloviar, S.; Joshi, S.; Klaus, J.; Kuhn, K.; Lavric, D.; Lu, M.; Mariappan, H.; Mistry, K.; Norris, B.; Rahhal-orabi, N.; Ranade, P.; Sandford, J.; Shifren, L.; Souw, V.; Tone, K.; Tambwe, F.; Thompson, A.; Towner, D.; Troeger, T.; Vandervoorn, P.; Wallace, C.; Wiedemer, J.; Wiegand, C. 45nm High-k + Metal Gate Strain-Enhanced Transistors. *2008 Symposium on VLSI Technology, 17−19 June, 2008*; 2008; pp 128−129.

(8) Auth, C.; Allen, C.; Blattner, A.; Bergstrom, D.; Brazier, M.; Bost, M.; Buehler, M.; Chikarmane, V.; Ghani, T.; Glassman, T.; Grover, R.; Han, W.; Hanken, D.; Hattendorf, M.; Hentges, P.; Heussner, R.; Hicks, J.; Ingerly, D.; Jain, P.; Jaloviar, S.; James, R.; Jones, D.; Jopling, J.; Joshi, S.; Kenyon, C.; Liu, H.; McFadden, R.; McIntyre, B.; Neirynck, J.; Parker, C.; Pipes, L.; Post, I.; Pradhan, S.; Prince, M.; Ramey, S.; Reynolds, T.; Roesler, J.; Sandford, J.; Seiple, J.; Smith, P.; Thomas, C.; Towner, D.; Troeger, T.; Weber, C.; Yashar, P.; Zawadzki, K.; Mistry, K. A 22nm High Performance and Low-Power CMOS Technology Featuring Fully-Depleted Tri-Gate Transistors, Self-Aligned Contacts and High Density MIM

DOI: 10.1021/acsami.9b12878
ACS Appl. Mater. Interfaces 2019, 11, 38929−38936

Capacitors. *2012 Symposium on VLSI Technology (VLSIT), 12−14 June, 2012*; 2012; pp 131−132.
(9) Park, M. H.; Lee, H. J.; Kim, G. H.; Kim, Y. J.; Kim, J. H.; Lee, J. H.; Hwang, C. S. Tristate Memory Using Ferroelectric−Insulator−Semiconductor Heterojunctions for 50% Increased Data Storage. *Adv. Funct. Mater.* **2011**, *21*, 4305−4313.
(10) Lee, D.; Jeon, B. C.; Baek, S. H.; Yang, S. M.; Shin, Y. J.; Kim, T. H.; Kim, Y. S.; Yoon, J.-G.; Eom, C. B.; Noh, T. W. Active Control of Ferroelectric Switching Using Defect-Dipole Engineering. *Adv. Mater.* **2012**, *24*, 6490−6495.
(11) Scott, J. F.; Dawber, M. Oxygen-Vacancy Ordering as a Fatigue Mechanism in Perovskite Ferroelectrics. *Appl. Phys. Lett.* **2000**, *76*, 3801−3803.
(12) Tagantsev, A. K.; Gerra, G. Interface-Induced Phenomena in Polarization Response of Ferroelectric Thin Films. *J. Appl. Phys.* **2006**, *100*, 051607.
(13) Chew, K.-H.; Ong, L.-H.; Osman, J.; Tilley, D. R. Hysteresis Loops of Ferroelectric Bilayers and Superlattices. *Appl. Phys. Lett.* **2000**, *77*, 2755−2757.
(14) Boni, G. A.; Filip, L. D.; Chirila, C.; Pasuk, I.; Negrea, R.; Pintilie, I.; Pintilie, L. Multiple Polarization States in Symmetric Ferroelectric Heterostructures for Multi-Bit Non-Volatile Memories. *Nanoscale* **2017**, *9*, 19271−19278.
(15) Lee, J. H.; Chu, K.; Kim, K.-E.; Seidel, J.; Yang, C.-H. Out-of-Plane Three-Stable-State Ferroelectric Switching: Finding the Missing Middle States. *Phys. Rev. B* **2016**, *93*, 115142.
(16) Baudry, L.; Lukyanchuk, I.; Vinokur, V. M. Ferroelectric Symmetry-Protected Multibit Memory Cell. *Sci. Rep.* **2017**, *7*, 42196.
(17) Damodaran, A. R.; Pandya, S.; Agar, J. C.; Cao, Y.; Vasudevan, R. K.; Xu, R.; Saremi, S.; Li, Q.; Kim, J.; McCarter, M. R.; Dedon, L. R.; Angsten, T.; Balke, N.; Jesse, S.; Asta, M.; Kalinin, S. V.; Martin, L. W. Three-State Ferroelastic Switching and Large Electromechanical Responses in PbTiO3 Thin Films. *Adv. Mater.* **2017**, *29*, 1702069.
(18) Xu, R.; Liu, S.; Saremi, S.; Gao, R.; Wang, J. J.; Hong, Z.; Lu, H.; Ghosh, A.; Pandya, S.; Bonturim, E.; Chen, Z. H.; Chen, L. Q.; Rappe, A. M.; Martin, L. W. Kinetic Control of Tunable Multi-state Switching in Ferroelectric Thin Films. *Nat. Commun.* **2019**, *10*, 1282.
(19) Roelofs, A.; Pertsev, N. A.; Waser, R.; Schlaphof, F.; Eng, L. M.; Ganpule, C.; Nagarajan, V.; Ramesh, R. Depolarizing-Field-Mediated 180° Switching in Ferroelectric Thin Films with 90° Domains. *Appl. Phys. Lett.* **2002**, *80*, 1424−1426.
(20) Nagarajan, V.; Roytburd, A.; Stanishevsky, A.; Prasertchoung, S.; Zhao, T.; Chen, L.; Melngailis, J.; Auciello, O.; Ramesh, R. Dynamics of Ferroelastic Domains in Ferroelectric Thin Films. *Nat. Mater.* **2003**, *2*, 43−47.
(21) Dawber, M.; Rabe, K. M.; Scott, J. F. Physics of Thin-Film Ferroelectric Oxides. *Rev. Mod. Phys.* **2005**, *77*, 1083−1130.
(22) Kalinin, S. V.; Rodriguez, B. J.; Borisevich, A. Y.; Baddorf, A. P.; Balke, N.; Chang, H. J.; Chen, L.-Q.; Choudhury, S.; Jesse, S.; Maksymovych, P.; Nikiforov, M. P.; Pennycook, S. J. Defect-Mediated Polarization Switching in Ferroelectrics and Related Materials: From Mesoscopic Mechanisms to Atomistic Control. *Adv. Mater.* **2010**, *22*, 314−322.
(23) Nelson, C. T.; Gao, P.; Jokisaari, J. R.; Heikes, C.; Adamo, C.; Melville, A.; Baek, S.-H.; Folkman, C. M.; Winchester, B.; Gu, Y.; Liu, Y.; Zhang, K.; Wang, E.; Li, J.; Chen, L.-Q.; Eom, C.-B.; Schlom, D. G.; Pan, X. Domain Dynamics During Ferroelectric Switching. *Science* **2011**, *334*, 968−971.
(24) Böscke, T. S.; Müller, J.; Bräuhaus, D.; Schröder, U.; Böttger, U. Ferroelectricity in Hafnium Oxide Thin Films. *Appl. Phys. Lett.* **2011**, *99*, 102903.
(25) Müller, J.; Böscke, T. S.; Schröder, U.; Mueller, S.; Bräuhaus, D.; Böttger, U.; Frey, L.; Mikolajick, T. Ferroelectricity in Simple Binary ZrO_2 and HfO_2. *Nano Lett.* **2012**, *12*, 4318−4323.
(26) Park, M. H.; Lee, Y. H.; Kim, H. J.; Kim, Y. J.; Moon, T.; Kim, K. D.; Müller, J.; Kersch, A.; Schroeder, U.; Mikolajick, T.; Hwang, C. S. Ferroelectricity and Antiferroelectricity of Doped Thin HfO_2-Based Films. *Adv. Mater.* **2015**, *27*, 1811−1831.
(27) Shimizu, T.; Katayama, K.; Kiguchi, T.; Akama, A.; Konno, T. J.; Sakata, O.; Funakubo, H. The Demonstration of Significant Ferroelectricity in Epitaxial Y-Doped HfO_2 Film. *Sci. Rep.* **2016**, *6*, 32931.
(28) Yurchuk, E.; Muller, J.; Hoffmann, R.; Paul, J.; Martin, D.; Boschke, R.; Schlosser, T.; Muller, S.; Slesazeck, S.; Bentum, R.; Trentzsch, M.; Schroder, U.; Mikolajick, T. HfO2-Based Ferroelectric Field-Effect Transistors with 260 nm Channel Length and Long Data Retention. *4th IEEE International Memory Workshop, 20−23 May, 2012*; 2012; pp 1−4.
(29) Muller, J.; Boscke, T. S.; Schroder, U.; Hoffmann, R.; Mikolajick, T.; Frey, L. Nanosecond Polarization Switching and Long Retention in a Novel MFIS-FET Based on Ferroelectric HfO2. *IEEE Electron Device Lett.* **2012**, *33*, 185−187.
(30) Lee, K.; Lee, T. Y.; Yang, S. M.; Lee, D. H.; Park, J.; Chae, S. C. Ferroelectricity in Epitaxial Y-Doped HfO_2 Thin Film Integrated on Si Substrate. *Appl. Phys. Lett.* **2018**, *112*, 202901.
(31) Mulaosmanovic, H.; Slesazeck, S.; Ocker, J.; Pesic, M.; Muller, S.; Flachowsky, S.; Müller, J.; Polakowski, P.; Paul, J.; Jansen, S.; Kolodinski, S.; Richter, C.; Piontek, S.; Schenk, T.; Kersch, A.; Kunneth, C.; Bentum, R. v.; Schroder, U.; Mikolajick, T. Evidence of Single Domain Switching in Hafnium Oxide Based FeFETs: Enabler for Multi-Level FeFET Memory Cells. *2015 IEEE International Electron Devices Meeting (IEDM), 7−9 Dec., 2015*; 2015; pp 26.28.21−26.28.23
(32) Dünkel, S.; Trentzsch, M.; Richter, R.; Moll, P.; Fuchs, C.; Gehring, O.; Majer, M.; Wittek, S.; Müller, B.; Melde, T.; Mulaosmanovic, H.; Slesazeck, S.; Müller, S.; Ocker, J.; Noack, M.; Löhr, D.; Polakowski, P.; Müller, J.; Mikolajick, T.; Höntschel, J.; Rice, B.; Pellerin, J.; Beyer, S. A FeFET Based Super-Low-Power Ultra-Fast Embedded NVM Technology for 22nm FDSOI and Beyond. *2017 IEEE International Electron Devices Meeting (IEDM), 2−6 Dec., 2017*; 2017; pp 19.17.11−19.17.14.
(33) Mulaosmanovic, H.; Ocker, J.; Müller, S.; Noack, M.; Müller, J.; Polakowski, P.; Mikolajick, T.; Slesazeck, S. Novel Ferroelectric FET Based Synapse for Neuromorphic Systems. *2017 Symposium on VLSI Technology, 5−8 June, 2017*; 2017; pp T176−T177.
(34) Oh, S.; Kim, T.; Kwak, M.; Song, J.; Woo, J.; Jeon, S.; Yoo, I. K.; Hwang, H. $HfZrO_x$-Based Ferroelectric Synapse Device With 32 Levels of Conductance States for Neuromorphic Applications. *IEEE Electron Device Lett.* **2017**, *38*, 732−735.
(35) Chen, L.; Wang, T.-Y.; Dai, Y.-W.; Cha, M.-Y.; Zhu, H.; Sun, Q.-Q.; Ding, S.-J.; Zhou, P.; Chua, L.; Zhang, D. W. Ultra-Low Power $Hf_{0.5}Zr_{0.5}O_2$ Based Ferroelectric Tunnel Junction Synapses for Hardware Neural Network Applications. *Nanoscale* **2018**, *10*, 15826−15833.
(36) Mulaosmanovic, H.; Mikolajick, T.; Slesazeck, S. Random Number Generation Based on Ferroelectric Switching. *IEEE Electron Device Lett.* **2018**, *39*, 135−138.
(37) Seo, M.; Kang, M.-H.; Jeon, S.-B.; Bae, H.; Hur, J.; Jang, B. C.; Yun, S.; Cho, S.; Kim, W.-K.; Kim, M.-S.; Hwang, K.-M.; Hong, S.; Choi, S.-Y.; Choi, Y.-K. First Demonstration of a Logic-Process Compatible Junctionless Ferroelectric FinFET Synapse for Neuromorphic Applications. *IEEE Electron Device Lett.* **2018**, *39*, 1445−1448.
(38) Lee, T. Y.; Lee, K.; Lim, H. H.; Song, M. S.; Yang, S. M.; Yoo, H. K.; Suh, D. I.; Zhu, Z.; Yoon, A.; MacDonald, M. R.; Lei, X.; Jeong, H. Y.; Lee, D.; Park, K.; Park, J.; Chae, S. C. Ferroelectric Polarization-Switching Dynamics and Wake-Up Effect in Si-Doped HfO2. *ACS Appl. Mater. Interfaces* **2018**, *11*, 3142−3149.
(39) Yamaguchi, M.; Fujii, S.; Kamimuta, Y.; Kabuyanagi, S.; Ino, T.; Nakasaki, Y.; Takaishi, R.; Ichihara, R.; Saitoh, M. Impact of Specific Failure Mechanisms on Endurance Improvement for HfO_2-based Ferroelectric Tunnel Junction Memory. *2018 IEEE International Reliability Physics Symposium (IRPS), 11−15 March, ≪2018*; 2018; pp 6D.2-1−6D.2-6.
(40) Lu, Y.; Alvarez, A.; Kao, C.-H.; Bow, J.-S.; Chen, S.-Y.; Chen, I.-W. An Electronic Silicon-Based Memristor with a High Switching Uniformity. *Nat. Electron.* **2019**, *2*, 66−74.

DOI: 10.1021/acsami.9b12878
ACS Appl. Mater. Interfaces 2019, 11, 38929−38936

(41) Jo, J. Y.; Han, H. S.; Yoon, J.-G.; Song, T. K.; Kim, S.-H.; Noh, T. W. Domain Switching Kinetics in Disordered Ferroelectric Thin Films. *Phys. Rev. Lett.* **2007**, *99*, 267602.
(42) Merz, W. J. Domain Formation and Domain Wall Motions in Ferroelectric BaTiO3 Single Crystals. *Phys. Rev.* **1954**, *95*, 690−698.
(43) Alessandri, C.; Pandey, P.; Abusleme, A.; Seabaugh, A. Switching Dynamics of Ferroelectric Zr-Doped HfO_2. *IEEE Electron Device Lett.* **2018**, *39*, 1780−1783.
(44) So, Y. W.; Kim, D. J.; Noh, T. W.; Yoon, J.-G.; Song, T. K. Polarization Switching Kinetics of Epitaxial $Pb(Zr_{0.4}Ti_{0.6})O_3$ Thin Films. *Appl. Phys. Lett.* **2005**, *86*, 092905.
(45) Jo, J. Y.; Yang, S. M.; Kim, T. H.; Lee, H. N.; Yoon, J.-G.; Park, S.; Jo, Y.; Jung, M. H.; Noh, T. W. Nonlinear Dynamics of Domain-Wall Propagation in Epitaxial Ferroelectric Thin Films. *Phys. Rev. Lett.* **2009**, *102*, 045701.
(46) Guo, E. J.; Dörr, K.; Herklotz, A. Strain Controlled Ferroelectric Switching Time of $BiFeO_3$ Capacitors. *Appl. Phys. Lett.* **2012**, *101*, 242908.
(47) Fu, D.; Suzuki, K.; Kato, K.; Suzuki, H. Dynamics of Nanoscale Polarization Backswitching in Tetragonal Lead Zirconate Titanate Thin Film. *Appl. Phys. Lett.* **2003**, *82*, 2130−2132.
(48) Kang, B. S.; Yoon, J.-G.; Kim, D. J.; Noh, T. W.; Song, T. K.; Lee, Y. K.; Lee, J. K.; Park, Y. S. Mechanisms for Retention loss in Ferroelectric $Pt/Pb(Zr_{0.4}Ti_{0.6})O_3/Pt$ Capacitors. *Appl. Phys. Lett.* **2003**, *82*, 2124−2126.
(49) Kang, B. S.; Yoon, J.-G.; Noh, T. W.; Song, T. K.; Seo, S.; Lee, Y. K.; Lee, J. K. Polarization Dynamics and Retention Loss in Fatigued $PbZr_{0.4}Ti_{0.6}O_3$ Ferroelectric Capacitors. *Appl. Phys. Lett.* **2003**, *82*, 248−250.
(50) Fengler, F. P. G.; Hoffmann, M.; Slesazeck, S.; Mikolajick, T.; Schroeder, U. On the Relationship Between Field Cycling and Imprint in Ferroelectric $Hf_{0.5}Zr_{0.5}O_2$. *J. Appl. Phys.* **2018**, *123*, 204101.
(51) Ishibashi, Y. Theory of Polarization Reversals in Ferroelectrics Based on Landau-Type Free Energy. *Jpn. J. Appl. Phys.* **1992**, *31*, 2822−2824.
(52) Vopsaroiu, M.; Blackburn, J.; Cain, M. G.; Weaver, P. M. Thermally Activated Switching Kinetics in Second-Order Phase Transition Ferroelectrics. *Phys. Rev. B: Condens. Matter Mater. Phys.* **2010**, *82*, 024109.
(53) Clima, S.; Wouters, D. J.; Adelmann, C.; Schenk, T.; Schroeder, U.; Jurczak, M.; Pourtois, G. Identification of the Ferroelectric Switching Process and Dopant-Dependent Switching Properties in Orthorhombic HfO_2: A First Principles Insight. *Appl. Phys. Lett.* **2014**, *104*, 092906.
(54) Zhou, D.; Guan, Y.; Vopson, M. M.; Xu, J.; Liang, H.; Cao, F.; Dong, X.; Mueller, J.; Schenk, T.; Schroeder, U. Electric Field and Temperature Scaling of Polarization Reversal in Silicon Doped Hafnium Oxide Ferroelectric Thin Films. *Acta Mater.* **2015**, *99*, 240−246.
(55) Nomura, Y.; Tachi, T.; Kawae, T.; Morimoto, A. Temperature Dependence of Ferroelectric Properties and the Activation Energy of Polarization Reversal in (Pr,Mn)-Codoped $BiFeO_3$ Thin Films. *Phys. Status Solidi B* **2015**, *252*, 833−838.
(56) Tybell, T.; Paruch, P.; Giamarchi, T.; Triscone, J.-M. Domain Wall Creep in Epitaxial Ferroelectric $Pb(Zr_{0.2}Ti_{0.8})O_3$ Thin Films. *Phys. Rev. Lett.* **2002**, *89*, 097601.
(57) Chen, Y. C.; Lin, Q. R.; Chu, Y. H. Domain Growth Dynamics in Single-Domain-like $BiFeO_3$ Thin Films. *Appl. Phys. Lett.* **2009**, *94*, 122908.
(58) Son, J. Y.; Park, C. S.; Kim, S.-K.; Shin, Y.-H. Writing Ferroelectric Domain Bits on the $PbZr_{0.48}Ti_{0.52}O_3$ thin film. *J. Appl. Phys.* **2008**, *104*, 064101.
(59) Kim, Y.; Kim, W.; Choi, H.; Hong, S.; Ko, H.; Lee, H.; No, K. Nanoscale Domain Growth Dynamics of Ferroelectric Poly-(vinylidene fluoride-co-trifluoroethylene) Thin Films. *Appl. Phys. Lett.* **2010**, *96*, 012908.
(60) Buragohain, P.; Richter, C.; Schenk, T.; Lu, H.; Mikolajick, T.; Schroeder, U.; Gruverman, A. Nanoscopic Studies of Domain Structure Dynamics in Ferroelectric La:HfO_2 Capacitors. *Appl. Phys. Lett.* **2018**, *112*, 222901.
(61) Wu, Y.-Z.; Yao, D.-L.; Li, Z.-Y. Monte-Carlo Simulation of the Switching Behavior in Ferroelectrics with Dipolar Defects. *Solid State Commun.* **2002**, *122*, 395−400.
(62) Schenk, T.; Hoffmann, M.; Ocker, J.; Pešić, M.; Mikolajick, T.; Schroeder, U. Complex Internal Bias Fields in Ferroelectric Hafnium Oxide. *ACS Appl. Mater. Interfaces* **2015**, *7*, 20224−20233.
(63) Pešić, M.; Fengler, F. P. G.; Larcher, L.; Padovani, A.; Schenk, T.; Grimley, E. D.; Sang, X.; LeBeau, J. M.; Slesazeck, S.; Schroeder, U.; Mikolajick, T. Physical Mechanisms behind the Field-Cycling Behavior of HfO_2-Based Ferroelectric Capacitors. *Adv. Funct. Mater.* **2016**, *26*, 4601−4612.

DOI: 10.1021/acsami.9b12878
ACS Appl. Mater. Interfaces 2019, 11, 38929−38936